LETTERS

Stacking Faults in Formation of Silver Nanodisks

V. Germain,[†] Jing Li,[‡] D. Ingert,[†] Z. L. Wang,*,[‡] and M. P. Pileni*,[†]

*Laboratoire LM2N., Université Pierre et Marie Curie (Paris VI), B.P. 52, 4 Place Jussieu,
F-752 31 Paris Cedex 05, France, and School of Materials Science and Engineering,
Georgia Institute of Technology, Atlanta, Georgia 30332-0245*

Structural investigations by using high-resolution transmission electron microscopy (HRTEM) and selected area electron diffraction (SAED) of silver nanodisks with different sizes are presented. The disks have a face centered cubic (fcc) crystal structure and their flat surfaces are (111). Stacking faults parallel to the (111) planes are frequently observed for the nanodisks. A unique (111) stacking fault model which is parallel to the flat (111) disk surface has been proposed to explain the observed 1/3{422} forbidden reflections in [111] SAED pattern and the corresponding 3×{422} supperlattice fringes in the [111] HRTEM image. It is suggested that the presence of the stacking faults may be the key in the formation and growth of the disk morphology. This study may provide an insight to synthetically controlling particle shape and size through defect engineering.

In the past few years, research on inorganic nanocrystals has had a tremendous development because of their great potential for applications. This involves biology, electronics, transport, and information technology and implies producing nanocrystals with well-defined sizes, shapes, and crystallinity. Several challenges have to be faced. We must produce large amounts and well-controlled materials and be able to manipulate these nanocrystals. Several approaches[1] to produce these nanomaterials with various shapes have been undertaken in the past decade. Transmission electron microscopy is a powerful and unique technique for structure characterization.[2]

It is well-known that the physical and chemical properties of the nanoscale crystals are usually closely related to the nanoparticle shape and size. For this reason, the shape- and size-controlled procedure during the nanoparticles synthesis has become a new and interesting research focus. Very recently, several groups have made nanodisks morphology particles.[3-7] The silver nanoprisms with the perfectly triangular and truncated triangular shapes,[4] as well as the silver nanodisks with truncated

triangular and hexagonal shapes,[5] have been synthesized using different methods. These silver nanoprisms and nanodisks have the optical properties different from the silver nanospheres and have a potential application in optics.[4,5] We have been able to tune the silver nanodisk size from 30 to 120 nm,[8] resulting in drastic changes in the optical properties.
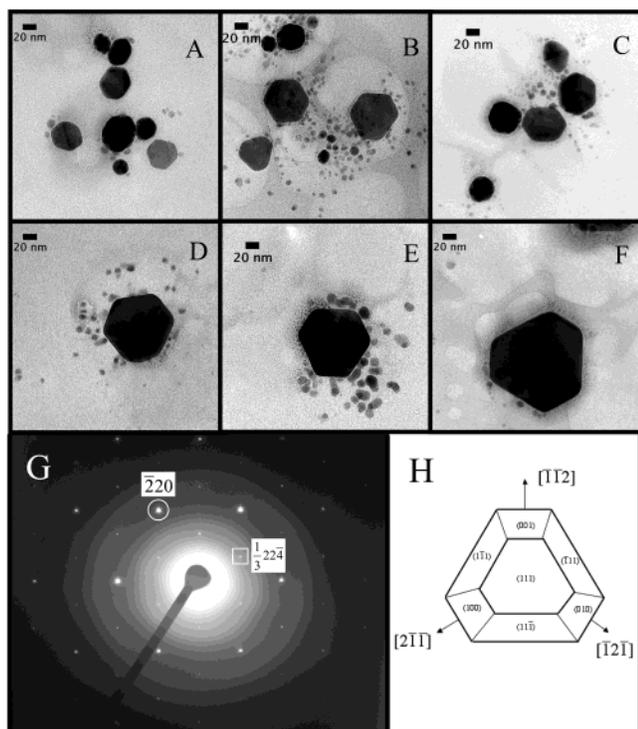
Both silver nanoprisms and nanodisks mentioned above synthesized by different groups using different methods have a flat platelike shape with the flat top surface parallel to the (111) plane of their fcc crystal structure. Also, both show the presence of the 1/3{422} reflections in the [111] electron diffraction pattern,[4,5] which should be forbidden for perfect fcc structure. This phenomenon has been observed by many authors in Au or Ag platelike crystals, and a number of explanations for the occurrence of such forbidden reflections have been previously suggested,[3,9-12] which will be elaborated in below.

In this paper, based on detailed structure characterization for the silver nanodisks with different sizes by using HRTEM and SAED analyses, we give an alternative explanation about the formation of these 1/3{422} forbidden reflections: It is the (111) stacking faults lying parallel to the (111) surface and extending across the entire disk that are responsible for creating the

---

* To whom correspondence should be addressed.
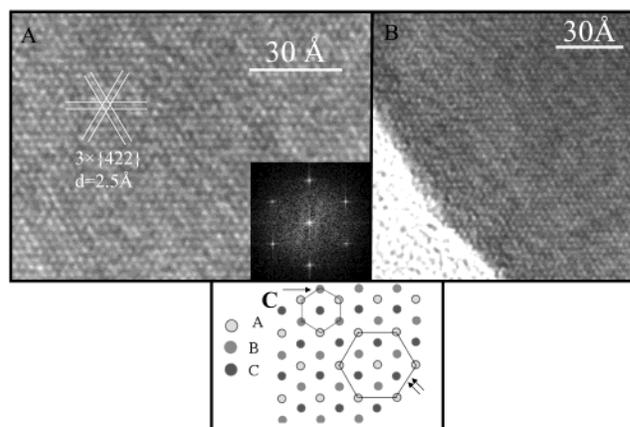† Université Pierre et Marie Curie (Paris VI).
‡ Georgia Institute of Technology.

Figure 1. TEM images of silver nanodisks. From A to F the hydrazine content increases from $r = 4.7$ to 11.8. (A) $r = 4.7$, (B) $r = 6.3$, (C) $= 7.1$, (D) $r = 7.9$, (E) $r = 9.8$, (F) $= 11.8$, (G) Schematic drawing of a typical nanodisk with the crystallographic orientation. (H) A typical [111] SAED pattern of silver nanodisk in the sample E. The bright spots correspond to the {220} Bragg reflections, and the circled spot is $\overline{2}20$. The weaker spots closer to the center are attributed to 1/3{422} forbidden reflections; the boxed spot is 1/3 $22\overline{4}$.
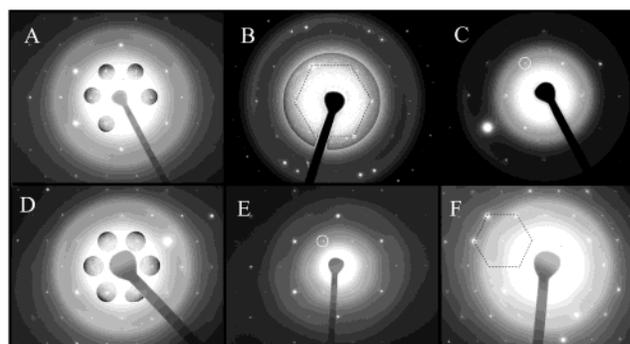
1/3{422} reflections in the [111] pattern. We also propose that the stacking faults play an important role for the formation and growth of the platelike silver nanodisks. This will provide an insight to synthetically controlling particle shape and size through defect design.

The nanodisk sizes are tuned by the amount of reducing agent added during the synthesis (see Appendix I). Figure 1 shows the TEM[13] images for 6 different samples differing by their sizes. Sphericals and highly faceted large particles with a rather wide size distribution are produced (Figure 1). In the following, we will concentrate our effort on the large and faceted nanocrystals.

Figure 1G shows the selected area electron diffraction (SAED) pattern from the sample shown in Figure 1E. The electron beam was perpendicular to the flat surface of the disk lying on the TEM grid. The diffraction pattern exhibits 6 bright and sharp spots in a 6-fold symmetry corresponding to the {220} reflections of the fcc silver single-crystal orientated in the [111] direction, indicating that the flat surface of the disks is parallel to the (111) habit plane. In previous work,[5] the crystallography of the disk is described as a flat (111) face on the top with truncated faces as shown in Figure 1H. Figure 2A shows a HRTEM image of the [111] orientated disk (same sample as in Figure 2) with his flat (111) plane lying on TEM grid. The image shows a perfect lattice and exhibits 6-fold symmetry. This is well demonstrated by the Fourier transform shown in the insert of Figure 2A. The lattice spacing is 2.50 Å, corresponding to the 3 × {422} lattice spacing of the fcc silver crystal which can be built by 3 sets of 3 × {422} spacing. In the following, we name these fringes as 3 × {422} supperlattice fringes. This HRTEM observation is consistent with the diffraction pattern
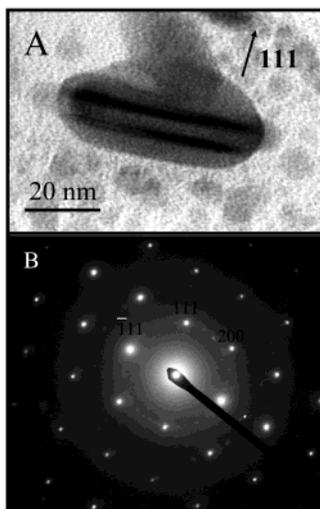

Figure 2. (A) HRTEM image at 400 kV of a silver nanodisk in the [111] orientation (sample E). The measured distance is three times the distance of {422}. In the insert, Fourier transform of the same area. (B) [111] HRTEM image of silver nanodisk at the edge region of the disk. The 3 × {422} fringes extend over the edge area. (C) Sketch of the fcc stacking of 3 layers of atoms along the [111] direction. The projected positions of the A atoms build a bigger unit cell (3 × {422} distance).

Figure 3. SAED patterns for all samples. All patterns show the 1/3{422} forbidden reflections. In Figure 4, parts A, B, and D, the 1/3{422} forbidden reflections occur in the circles in which the image contrast was adjusted. In Figure 4, parts B and F, the hexagonal box marked the 1/3{422} forbidden reflections. (Note: In Figure 4B the pattern does not come from one nanodisk; therefore, the pattern is not as perfect as others; but the same periodicity as marked by the hexagonal box caused by the 1/3{422} forbidden reflections is still visible.) In Figure 4, parts C and E one of the 1/3{422} forbidden reflections is marked by the circle.

given in Figure 1H, showing a relationship between reciprocal space and real space. This HRTEM image is not expected for a regular [111] HRTEM image of the fcc crystal. Usually, the [111] HRTEM image of the fcc crystal is built by 3 sets of the {220} spacing with a 6-fold symmetry. For silver, the {220} d spacing is 1.44 Å. Because this interfringe distance is beyond the resolution of our microscope, the [111] HRTEM image of the silver crystal will be not observable. However, for these samples, HRTEM images built by 3 sets of 3 × {422} spacing were frequently observed, this indicated that there is a superlattice caused by a bigger periodicity than a regular [111] unite cell. We have observed that these 3 × {422} fringes have the following features: (a) They build a perfect lattice and extend across the entire disk, include the region with a thickness gradient (for example, at the edge of the disks, see the Figure 3B); (b) There is not any isolated "island" in the entire image which do not show these 3 × {422} fringes.

In Figure 1H, the diffraction pattern shows 1/3{422} reflections (as marked by the box) which are formally forbidden for the perfect fcc structure. This observation is the same as those

Letters

J. Phys. Chem. B, Vol. 107, No. 34, 2003 **8719**

Figure 4. (A) TEM image of the silver nanodisk taken in side view, showing the contrast from (111) stacking faults and a preferential growth along the stacking faults. The orientation relationship of the SAED pattern and the nanodisk is shown in Figure 3, parts A and B. (B) A typical SAED pattern of silver nanodisk at 100 kV in the [01$\bar{1}$] orientation (side view).

that have been observed in previous work for these silver nanodisks[5] as well as in the silver nanoprism.[4] In Figure 3, the SAED of the 6 samples showing the same spots is presented. However, it can be note that the intensities differ from one sample to other. The 1/3{422} forbidden reflections on the [111] SAED pattern have been observed previously in platelike Au and Ag nanocrystals.[3,4,9−12] Figure 4A shows the TEM images of disks in side view. The typical [01$\bar{1}$] SAED pattern obtained for a beam direction parallel to the (111) disk surface is shown in Figure 4B.

A number of models for the occurrence of such forbidden reflections have been previously suggested[3,9−12] (see Appendix II). Model 1 can be excluded because all over the nanodisk the same lattice parameter is observed, whereas it is not the case for a fractional unit cell along [111] direction. Models[3,10,17] 2, 3, and 4 involve a twin parallel to the flat surface and can be ruled out because the SAED in the [01$\bar{1}$] direction does not exhibit a mirror symmetry (Figure 4B) as expected for twins parallel to the 111 face. Model 5 could explain the above observation. However, it requires a spacing between twins in the order of ~1 nm. Figure 4A shows a spacing of 5 nm, a value far away from the 1 nm required. From these data presence of twins can be rejected as a large density of stacking fault.

Let consider two types of stacking fault. (i) Stacking fault I (intrinsic):[18] An A layer is removed and the stacking sequence is then ABCBCABCABC... In this case the projected potential in A positions will be lower than that in B and C positions by one atom. (ii) Stacking fault II (extrinsic): An A layer is added that means the insertion of an extra (111) layer (for instance, the A layer) into the regular stacking sequence of ABCAB-CABC ..., a sequence of AB(A)CABCABC...will be caused. In this case, the projected potential in A positions will be higher than that in B and C positions by one atom.

For a single stacking fault, a strong supperlattice (or forbidden) diffraction effect could be induced, similar to the effect caused by a single surface mono-atomic step as mentioned in the model 1.[9] Because of the subnanometer thickness of the stacking fault, their reciprocal points are strongly elongated along the [111] direction. Therefore, they are very easy to

intersect with the Ewald sphere, and the 1/3{422} reflections will be very easy to observe in the [111] diffraction pattern. It is impossible to distinguish between these two models because in both cases the projected crystal potential along [111] is identical. The model described above is for a single stacking fault. If two or more (111) stacking faults exist within the nanodisk, because a different stacking fault will produce the same supperlattice periodicity, the same effect will appear in the HRTEM image and diffraction pattern, unless there are three stacking faults produced by intrinsic/extrinsic of A, B, and C layers, respectively.

The change in the intensity of the 1/3{422} forbidden reflections observed with various samples (Figure 3) is due to the fact that the intensity of the 3 × {422} supperlattice fringes depend on the different stacking sequence and thickness of the disks. By adjusting the [111] stacking sequence, the projected potential of the 3 × {422} superlattice changes and this results in different intensities of 1/3{422} forbidden reflections.

At this step, there is still one question open: is there a link between the stacking fault and the disk growth? We propose that the (111) stacking fault(s) play an important role to the formation and growth of the (111) disk. It is likely that the growth in parallel to the stacking fault plane is the fastest, and the existence of the stacking fault may be the key for the formation and growth of the diskette morphology. This has been confirmed by Figure 4A, in which the (111) stacking fault planes are apparent. The silver nanodisks observed in six of our samples are directly related to the presence of (111) stacking faults. A similar example has been reported by other authors:[14] The (111) microtwins play an important role in the evolution of the microstructure of the nano-Ge precipitates in Al−Ge and Ag−Ge alloys; An accelerated growth along the (111) twin plane leads to triangular or hexagonal nanoplate precipitates. We also suggest that the (111) stacking fault model proposed here could be applied to the work reported by others.[4] That work reported the photoinduced conversion of silver nanospheres to nanoprisms. The silver nanoprisms were formed from the small spherical silver particles in the colloidal suspension and grow with increased fluorescent irradiation. The similar [111] diffraction pattern with 1/3{422} forbidden reflections was reported for their silver nanoprisms. We suggest that photo irradiation induced (111) stacking fault in small silver particles and the growth was accelerated along (111) stacking fault, resulting in the formation of the triangle silver nanoprisms.

In this letter, the structural study of silver nanodisks differing by their sizes is presented. The nanodisks have a fcc crystal structure with (111) stacking fault(s) lying parallel to the (111) surface and extending across entire disk. We highlight that the (111) stacking fault is the reason for the occurrence of the 1/3{422} forbidden reflections and the 3 × {422} superlatice fringes. We conclude that the stacking faults may be the key for the formation and growth of the nanodisks. Therefore, by controlling the nucleation, growth, and elimination of the defect (stacking fault), the shape and size controlling of the nanocrystal will be possible. This will provide an insight to the synthetically controlling particle shape and size of the nanocrystals.

Appendix I

The nanodisks are obtained using the method described by Maillard and al.[8] Briefly, a micellar solution of 60% 0.1 M Ag(AOT)[15] and 40% 0.1 M Na(AOT)[15] (AOT= 2 ethyl-hexyl suffossucinate) with a water content $w = [H_2O]/[AOT] = 2$ is mixed with 0.1M Na(AOT) solution. The nanocrystals are coated with dodecanethiol (40 μl per mL) and extracted from

the solution. The hydrazine[16] content, r, defined as the ratio $[N_2H_4]/[AOT]$, varying from 4.7 to 11.8, controls the nanodisk size.

Appendix II

A brief summary is given as follows. For easy presentation, the fcc structure is taken as a stacking of hexagonal close-packed (111) layers along the [111] direction following a sequence of ABCABCABC..., where A, B, and C represent the three possible stacking positions for the (111) planes.

Model 1. For a perfect crystal with clean surfaces, mono-atomic surface steps on the (111) surface, which caused a fractional unit cell along the [111] direction and resulted in an incomplete ABC stacking sequence, break the regular fcc interference pattern and give rise to the 1/3{422} reflections.[9]

Model 2. For the platelets containing a single twin on the (111) plane parallel to the upper and lower (111) surface of the plate, if the number of (111) layers is not equal to 3n (n is an integer), the 1/3{422} forbidden reflections will appear; otherwise not. (In this model the (111) twin boundary is not in the center of the crystal.)[3,10]

Model 3. The effect on HRTEM image and diffraction pattern caused by a twin in the fcc bicrystalline silicon nanowires has been reported.[17] When the twin boundary lies parallel to the surface and perpendicular to electron beam and the twin boundary is in the center of the crystal (central twin), the 1/3{422} forbidden reflections and 3 × {422} fringes appear.

Model 4. Two or more parallel twins on (111) planes which are parallel to the upper and lower surface will always cause the 1/3{422} forbidden reflections, regardless the number of the (111) layers.[3,10]

Model 5. High-density stacking faults on (111) plane could form microtwins. For example, the insertion of one extra (111) layer (such as the B layer) causes a stacking sequence of ABC-(B)ABCABC.... Here, the ABC(B)A is a twin-like thin slide. In this case, the reciprocal lattice points in the first-order Laue zone will be elongated because of the shape factor introduced by the very thin twin-like layer, and the 1/3{422} reflections may appear in a [111] pattern.[1]

Model 6. Surface reconstruction may results in extra reflections.[12] However, surface reconstruction can only be easily observed for a clean surface under ultrahigh vacuum condition. For our sample synthesized in solution and passivated with polymer, we can rule out the possibility.

References and Notes

(1) Pileni, M. P. *Nature Mater.* **2003**, *2*, 145−150.

(2) Wang, Z. L. *J. Phys. Chem*. **2000**, *104*, 1153.

(3) Kirkland, A. I.; Jefferson, D. A.; Duff, D. G.; Edwards, P. P.; Gameson, I.; Johnson, B. F. G.; Smith, D. J. *Proc. R. Soc. London A* **1993**, *440*, 589−609.

(4) Jin, R.; Cao, Y.W.; Mirkin, C. A.; Kelly, K. L.; Schatz, G. C.; Zheng, J. G. *Science* **2001**, *294*, 1901.

(5) Maillard, M.; Giorgio, S.; Pileni, M. P. *Adv. Mater.* **2002**, *14, 15,* 1084.

(6) Chen, S.; Fan, Z.; Carroll, D. L. *J. Phys. Chem*. **2002**, *106*, 10777.

(7) Pastoriza-Santos, I.; Liz-Marzan, M. L. *Nano Lett.* **2002**, *2*, 903.

(8) Maillard, M.; Giorgio, S.; Pileni, M. P. *J. Phys. Chem.* **2003**, *107*, 11, 1466−2470.

(9) Cherns, D. *Philos. Mag.* 1**974**, *30*, 549.

(10) Kirkland, A. I.; Jefferson, D. A.; Duff, D. G.; Edwards, P. P. *Inst. Phys. Conf. Ser*. **1989**, *98*, 375.

(11) Tanaka, N.; Cowley, J. M. *Mater. Res. Soc. Symp. Proc.* **1985**, *41*, 155

(12) Heyraud, J. C.; Métois, J. J. *Surf. Sci.* **1980**, *100*, 519.

(13) TEM images at moderate resolution and SAED patterns were recorded using a Hitachi HF-2000 field emission gun (FEG) transmission electron microscope (TEM) operating at 200 kV; and HRTEM was carried out using a JEOL 4000EX microscope operating at 400 kV.

(14) Dahmen, U.; Hethering, C. J. D.; Radmilovic, V.; Johnson, E. E. J.; Xiao, S. Q.; Luo, C. P. *Proc. 15th Int. Congr. Electron. Microsc.* **2002**, 131.

(15) Petit, C.; Lixon, P.; Pileni, M. P. *J. Phys. Chem.* **1993**, *97*, 12974.

(16) Sodium di(2-ethyl-hexyl)sulfoccinate Na(AOT), isooctane, hydrazine and dodecanethiol were from Sigma, Fluka, Prolabo (France) and Janssen Chemicals, respectively. The products were used without further purification.

(17) Carim, A. H.; Lew, K. K.; Redwing, J. M. *Adv. Mater.* **2001**, 1489.

(18) Hirsch, P.; Howie, A.; Nicholson, R. B.; Pashley, D. W.; Whelan, M. J. *Electron Microscopy of Thin Crystals*; Robert E. Krieger Publishing Company: New York, 1977.